

(4-CH₃). Anal. Calcd for C₂₁H₂₈CrO₄: C, 63.62; H, 7.12. Found: C, 63.05; H, 7.32.

X-ray Crystallography. Crystals of (C₆Et₅COCH₃)Cr(CO)₃ were grown from CH₂Cl₂/heptane. The density was determined by suspension in an aqueous solution of ZnCl₂. Clear yellow parallelepiped crystals were examined under a polarizing microscope for homogeneity. A well-formed crystal, 0.55 × 0.45 × 0.16 mm, was selected and sealed in a Lindemann capillary. Unit cell parameters were obtained from a least-squares fit of χ , ϕ , and 2θ for 15 reflections in the range 20.8° < 2θ < 26.1° recorded on a Nicolet P3 diffractometer with use of graphite monochromated Mo K α radiation ($\lambda = 0.71069 \text{ \AA}$ at 22 °C). Intensity data were also recorded on a Nicolet P3 diffractometer with a coupled $\theta(\text{crystal})-2\theta(\text{counter})$ scan, for 3003 reflections in the hemisphere ($h, \pm k, \pm l$) with $2\theta \leq 45^\circ$. The methods of selection of scan rates and initial data treatment have been described.^{16,17} Corrections for Lorentz-polarization effects and absorption (ψ scans)¹⁸ were applied to all reflections. Two standard reflections (5,-1,-2, 1.59%; and 2,-5,-2, 1.69%) monitored every 48 reflections showed no sign of crystal decomposition or instrument instability. Symmetry-equivalent data (330) were then averaged ($R_{\text{int}} = 0.0076$) to give 2673 unique reflections. A summary of crystal data is given in Table II.

Solution of the Structure. The coordinates of the chromium atom were found from a three-dimensional Patterson synthesis with use of the program SHELX-76.¹⁹ Full-matrix least-squares refinements followed by a three-dimensional electron density synthesis revealed all the non-hydrogen atoms. After refinement, the temperature factors of the non-hydrogen atoms, which were previously isotropic, were made anisotropic, and further cycles of refinement revealed the positional parameters for most of the hydrogen atoms. These were included in subsequent cycles of refinement along with the remaining hydrogen atoms fixed in their calculated positions, (U fixed at 0.08 \AA^2). Further refinement using full-matrix least squares minimizing $\sum w(|F_o| - |F_c|)^2$ was terminated

when the maximum shift/error reached 0.057. Final $R_1 = 0.0501$, $R_2 = 0.0547$ for 2198 reflections for which $I > 2.5\sigma(I)$. Correction for secondary extinction was not necessary. Throughout the refinement, scattering curves were taken from ref 20, and anomalous dispersion corrections from ref 21 were applied to the curve for chromium. All calculations were performed on a VAX 8650 computer. Programs used were as follows: XTAL,²² data reduction; TAPER,¹⁸ absorption correction; SHELX-76,¹⁹ structure solution and refinement; MOLGEOM,²³ molecular geometry; and SNOOPI,²⁴ diagrams. Final atomic positional parameters are given in Table III, selected bond lengths and bond angles are given in Table IV.

Acknowledgment. We thank the donors of the Petroleum Research Fund, administered by the American Chemical Society, for partial support of this research. Financial support from the Natural Sciences and Engineering Research Council of Canada is gratefully acknowledged. B.M. thanks the Ontario Provincial Government for an International Students Scholarship. Mass spectra were obtained courtesy of Dr. Richard W. Smith of the McMaster Regional Centre for Mass Spectrometry.

Registry No. 6, 77922-78-2; 7, 123674-42-0; Cr(CO)₆, 13007-92-6; hexaethylbenzene, 604-88-6.

Supplementary Material Available: Tables SI-SIV listing full crystal data, least-squares mean planes and dihedral/torsional angles, hydrogen atom positional parameters, and anisotropic temperature factors, respectively (7 pages); Table SV listing observed and calculated structure factors (5 pages). Ordering information is given on any current masthead page.

(16) Lippert, B.; Lock, C. J. L.; Rosenberg, B.; Zvagulis, M. *Inorg. Chem.* **1977**, *16*, 1525.

(17) Hughes, R. P.; Krishnamachari, N.; Lock, C. J. L.; Powell, J.; Turner, C. T. *Inorg. Chem.* **1977**, *16*, 314.

(18) Calabrese, J. C.; Burnett, R. M. TAPER locally modified by Z. Tun, with the permission of the Nicolet XRD Corp., 1980.

(19) Sheldrick, G. M. SHELX-76, Program for Crystal Structure Determination, University of Cambridge, England, 1976.

(20) Cromer, D. T.; Mann, J. B. *Acta Crystallogr.* **1968**, *A24*, 231.

(21) Cromer, D. T.; Liberman, D. *J. Chem. Phys.* **1970**, *53*, 1891.

(22) Stewart, J. M.; Hall, S. R. The XTAL System of Crystallographic Programs. Technical Report TR-1364, 1983; University of Maryland: College Park.

(23) Stephens, J. MOLGEOM adapted from CUDLS, McMaster University, Canada, 1973.

(24) Davies, K. CHEMGRAF suite: SNOOPI, Chemical Design Ltd. Oxford, England, 1983.

High-Temperature ²⁹Si NMR Investigation of Solid and Molten Silicates

I. Farnan* and J. F. Stebbins

Contribution from the Department of Geology, Stanford University, Stanford, California 94305. Received May 11, 1989

Abstract: High-temperature (up to 1250 °C) ²⁹Si NMR T_1 and line-shape measurements were made on silicate samples with varying SiO₂ contents. The samples represented a range of bridging and nonbridging oxygen distributions from Q⁴ in albite (NaAlSi₃O₈) to Q² and Q⁰ in a mixture of lithium orthosilicate and metasilicate (Li₄SiO₄/Li₂SiO₃). T_1 relaxation data as a function of temperature for glassy samples showed a dramatic increase in efficiency at the glass transition. This was ascribed to relaxation by paramagnetic impurities becoming more efficient as silicon atoms and impurity ions begin to diffuse through the material at temperatures above T_g . In each sample chemical exchange was observed at high temperature, indicating that the lifetime of a silicate tetrahedron in the melt is short on the NMR time scale, i.e., a few microseconds. Variable-temperature line-shape data for potassium tetrasilicate (K₂Si₄O₉) allowed the exchange process to be modelled and spectra to be simulated, yielding an activation energy for the process. This was in good agreement with the activation energy for viscous flow derived from viscosity measurements. It appears that ²⁹Si NMR is coming close to detecting the fundamental step in viscous flow in silicates with good agreement between the time constant of the exchange process determined by NMR and the shear relaxation time of the potassium tetrasilicate liquid.

Understanding of the physical chemistry of silicate liquids is important in both the earth sciences and material science: the chemical and physical behavior of magmas dominates many geological processes, and most technological glasses and glass ceramics start off in the molten state. Our present knowledge of

these systems is limited, however, by the technical difficulties of working at high temperatures, and the theoretical complexities of materials whose structure and dynamics lie somewhere between the relatively well-understood field of organic polymers and that of molten salts.

The ability of NMR measurements to give information about the dynamics of systems (as well as about their structure) through the measurement of relaxation times and line shapes over a range of temperature is well known. Here they have been applied over a temperature range of 1200 °C to silicate systems with different SiO₂ contents. There have been previous NMR measurements¹⁻³ on similar silicate systems covering a similar temperature range at a lower magnetic field. The purpose of this study was to improve the quality of the data, in terms of the signal-to-noise ratio, by building a more sensitive high-temperature probe and using a higher magnetic field (9.39 T). Data with improved signal to noise allows quantitative rather than qualitative measurements of the rates of motion and the higher magnetic field constrains the relaxation mechanism by its field dependence, something which was unclear from the previous experiments.

The motivation for these investigations is to understand the fundamental atomic scale processes which govern the macroscopic properties of silicate glasses and melts such as their viscosity and their bulk thermodynamic quantities. Most spectroscopic techniques (e.g., infrared and Raman spectroscopy) provide a "snapshot" view of the structure of a liquid because the time scale of the techniques is of the order of lattice vibrations. However, NMR can probe much lower frequency motions, motions which are important in the glass transition and the viscosity of a silicate liquid. In addition, the time scale of the NMR experiment may be varied (by changing the magnetic field, or the type of experiment, T_1 or $T_{1\rho}$, or observing quadrupolar effects) from a few hertz to several hundred megahertz. Most previous NMR studies of silicates at elevated temperatures have concentrated on non-network-forming cations.⁴ In this study, ²⁹Si NMR is used to observe the network-forming cation which should provide the most fundamental type of information.

²⁹Si NMR has shown previously in studies of glasses prepared with different quench rates⁵ that local structural information can be related to the configurational entropy of a silicate liquid. It is generally accepted that configurational considerations are one of the determining factors in the viscosity of glass-forming liquids.⁶ In order to understand more fully the behavior of natural magmas and many geological and technological processes, details of the atomic scale dynamics underlying the bulk properties of silicate liquids are required. Hopefully, the wealth of dynamic information about organic polymers gained by NMR studies can be extended to silicate systems.

Experimental Section

Samples were prepared with SiO₂ which was enriched to 95% in ²⁹Si (Oak Ridge National Laboratory) and high-purity Na₂CO₃, Al₂O₃, K₂CO₃, Li₂CO₃. These samples were albite (NaAlSi₃O₈) and potassium tetrasilicate (K₂Si₄O₉) glasses, and a mixture of crystalline lithium orthosilicate and metasilicate (Li₄SiO₄/Li₂SiO₃) with a near eutectic composition. Each represents a different bridging and nonbridging oxygen distribution, from framework Q⁴ (albite) to Q² and Q⁰ (lithium orthosilicate/metasilicate). In the Qⁿ nomenclature, *n* refers to the number oxygens per SiO₄ unit (Q) which are shared with another SiO₄ unit. The glass samples were made by heating stoichiometric amounts of their components to about 200 °C above the melting point for several hours; they were then quenched, reground, and remelted until homogeneous. The crystalline sample was made by slow cooling from the melt. In each preparation the weight loss at each stage was carefully monitored to ensure there was only negligible loss of alkalis.

The NMR data were recorded on a Varian VXR400S spectrometer (9.39 T) operating at 79.459 MHz for ²⁹Si. The high-temperature probe was home-built and consisted of a molybdenum furnace winding enclosed by alumina cement and alumina fiber-board insulation and a brass water

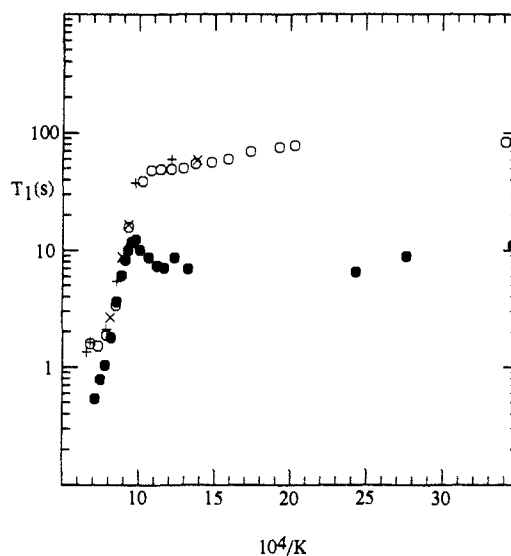


Figure 1. ²⁹Si T_1 versus inverse temperature for albite glass: the data of Liu et al.³ measured at 4.22 T (●); present data measured at 9.39 T with increasing temperature (○); measured with decreasing temperature (×); measured on a second experimental run (+). The error bars were less than the size of the symbols.

jacket. The NMR coil was also molybdenum and located at the center of the furnace on an alumina mount (i.e., at temperature) and was screened from the furnace by a shield of molybdenum foil which reduced the field due to the current in the windings to ~1.5 ppm. A polarity reversal switch on the furnace power supply allowed frequency shifts to be calibrated. The probe electronics were 6 cm from the rf coil and cooled by a large flow of room-temperature air. The tuning circuit was a simple tank circuit with a Q of ~110 at room temperature and ~9 at 1300 °C. Although the 90° pulse was 7 μs in ambient air it was limited to 14 μs by the blanket gas (Ar + 3% H₂) which broke down when the rf power was high. The gas was necessary to protect the molybdenum rf coil, shield, and furnace windings from oxidation at elevated temperatures. Low rf power is not a problem for silicon NMR in silicates since the spin-lattice relaxation times are long and the resonance is easily saturated for T_1 experiments, and the static line widths are modest and can be excited uniformly.

The NMR measurements were of two types; single pulse spectra and saturation recovery T_1 experiments. The T_1 data were collected following a saturation comb of 16 pulses with a series of 16 delays for temperatures where the relaxation times were greater than 10 s and 24 delays where relaxation was more rapid. Establishing the equilibrium magnetization for samples with long T_1 's requires a long experiment which raises the problem of the reaction of the sample with the sample container when held at high temperature for an extended amount of time. The small number of delays used here reflects our concern for maintaining the integrity of the sample throughout the experiment. The single-pulse spectra were all acquired with small-angle pulses and suitable delays to ensure there was no saturation of the resonance. Typically ~400 mg of sample was used in each experiment; this was contained in a sample container machined from high-purity boron nitride, which is only slightly reactive under reducing conditions and has excellent thermal conductivity. In each experiment the sample was recovered from the container as an intact pellet (i.e., it did not stick to the container walls), and the weight loss was less than 0.2 wt %. The room-temperature line shapes after the high-temperature runs were nearly identical with those of the starting material, indicating that compositional changes were insignificant. The sample temperature was calibrated separately from the experimental run using a thermocouple inside a sample container full of alumina powder. The sample temperature was then compared with the furnace control thermocouple temperature; using this method temperatures were reproducible within ±5 °C.

Results

Spin-Lattice Relaxation Times. The ²⁹Si T_1 relaxation times as a function of temperature for albite (NaAlSi₃O₈) are shown in Figure 1; the top curve is for the data reported here (9.39 T) and the lower curve that of Liu et al.² (4.22 T). The more informative portions of the T_1 curves are those above T_g where it would appear that the changes in T_1 are providing a probe of the motions which begin at T_g once enough energy is available

(1) Stebbins, J. F.; Murdoch, J. B.; Schneider, E.; Carmichael, I. S. E.; Pines, A. *Nature (London)* **1985**, *314*, 250-252.

(2) Liu, S.-B.; Pines, A.; Brandriss, M. E.; Stebbins, J. F. *Phys. Chem. Minerals* **1987**, *15*, 155-162.

(3) Liu, S.-B.; Stebbins, J. F.; Schneider, E.; Pines, A. *Geochim. Cosmochim. Acta* **1988**, *52*, 527-538.

(4) Müller-Warmuth, W.; Eckert, H. *Phys. Repts* **1982**, *88*, 91-149.

(5) Brandriss, M. E.; Stebbins, J. F. *Geochim. Cosmochim. Acta* **1988**, *52*, 2659-2669.

(6) Richet, P. *Geochim. Cosmochim. Acta* **1984**, *48*, 471-483.

for the previously "frozen in" structure to begin to rearrange itself again. Both data sets show good agreement with an apparent activation energy of the motion of 138.8 ± 8.6 and 131.4 ± 4.3 kJ mol⁻¹ for 9.39 and 4.22 T, respectively. There is a slight discrepancy between the curves with the lower field data showing a slight increase in T_1 just before the glass transition. This was attributed to the loss of some OH at ~ 500 °C leading to increased T_1 's because of the removal of the ¹H dipoles from the sample. Apart from this feature, below T_g the relaxation time varies very weakly with temperature, and its value is typical of the long T_1 's experienced by spectroscopists studying insulating materials using ²⁹Si NMR at room temperature. The T_1 relaxation times of high silica silicates are notoriously long (10's to 1000's of seconds); the proposed mechanism is relaxation by paramagnetic species, either impurities at the ppm level in glasses or, in the case of zeolites, atmospheric oxygen.⁷ The reason for this mechanism dominating the relaxation process is the weak coupling of the nuclear spin system to the lattice. The lack of any motion of the order of the Larmor frequency of the silicon nuclei, together with the small number of magnetic nuclei in natural abundance samples, means that the fluctuating magnetic field required to stimulate transitions in the spin system (and cause relaxation) is absent. Consequently, the fluctuating field due to the transitions of the unpaired electron (which is strongly coupled to the lattice) in the paramagnetic species together with spin diffusion provides a weak, but dominant relaxation mechanism. Paramagnetics such as Fe³⁺ and Mn²⁺ are often added in small amounts (<1000 ppm) to reduce the ²⁹Si relaxation times in these materials where there are problems in acquiring data in a reasonable amount of time. Small amounts (~ 1000 ppm) of strong dipoles such as ¹H have also been shown to reduce the ²⁹Si relaxation time in SiO₂ quite dramatically.⁸

The magnetic interaction responsible for the relaxation above T_g is not clear from the data, especially one set of data alone. The first interaction which suggests itself is a dipolar one between silicon nuclei, particularly in a sample enriched to 95% in ²⁹Si; this may be discounted in both sets of data by the strength of the interaction required to produce the minimum T_1 value. Assuming a model of random molecular motion, i.e., random angular modulation of a fixed dipole-dipole distance with a single correlation time, the dipolar interaction requires that the Si-Si distance be less than 1.1 Å between the confidence limits of the T_1 measurement. It was suggested by Liu et al.³ that relaxation may be caused by the formation of an intermediate or transition state which had an extreme chemical shift anisotropy and the silicon nuclei would relax owing to the rapid variation in the local field as they moved between states. The chemical shift anisotropy relaxation mechanism is dependent on the strength of the applied magnetic field; the rate ($1/T_1$) increases as the square of the magnetic field strength in the fast motion limit ($\omega_0\tau \ll 1$) and is linearly dependent⁹ on the magnetic field strength at the T_1 minimum ($\omega_0\tau \sim 1$). Consequently, if this were the mechanism, the minimum T_1 would be predicted by the 4.22 T data to be ~ 0.2 s at 9.39 T and not ~ 1.5 s as measured for albite. The relaxation interaction which remains as a possibility is the same as that at room temperature and below T_g , relaxation by paramagnetic impurities. The rapid increase in the efficiency of this mechanism at the glass transition is most probably due to the increased likelihood that a silicon atom will encounter a paramagnetic impurity as it diffuses or moves rapidly between configurations, or the paramagnetic impurities themselves may begin to diffuse through the structure. It is well known that in fast ion conductors the T_1 relaxation times can be dominated by paramagnetic effects when rapid diffusion of the conductor ions through the lattice occurs, and they can be relaxed by the strong fluctuating fields adjacent to a paramagnetic impurity.¹⁰

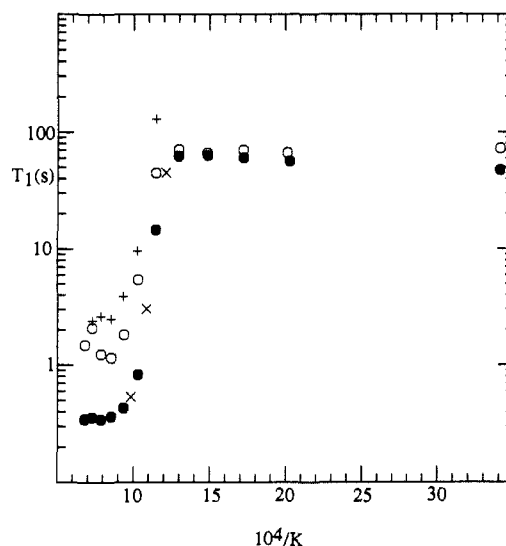


Figure 2. ²⁹Si T_1 versus inverse temperature for potassium tetrasilicate glass: undoped sample measured with increasing temperature (O), undoped sample measured with decreasing temperature (+); sample doped with 500 ppm Fe₂O₃ measured with increasing temperature (●); measured with decreasing temperature (×).

Figure 2 shows T_1 as a function of temperature for potassium tetrasilicate (K₂Si₄O₉). A sample of potassium tetrasilicate was also prepared containing 500 ppm of Fe₂O₃, the T_1 data for this sample are in the lower curve in Figure 2. The doped and undoped samples have a very similar T_1 behavior when the temperature is increased up to T_g , which may be surprising for the undoped sample has an impurity level which would be estimated, conservatively, to be <50 ppm of Fe³⁺. The water content of the sample is something which is very difficult to quantify, and the presence of strong ¹H dipoles in the structure would provide an alternative relaxation mechanism. The undoped sample exhibits some hysteresis when coming back down in temperature, but the doped sample shows quite reproducible behavior. Both doped and undoped samples show some two-component behavior at room temperature and at ~ 220 °C with slightly different relaxation times for Q³ and Q⁴ sites (107.1 and 72.7 s for undoped; 59.0 and 47.4 s for doped). The two-component behavior was present after the experimental run. At room temperature the doped sample T_1 's had increased by 6–7%; the undoped sample had T_1 's in excess of 500 s. This result is surprising in two respects: the Q³ silicons seem to have a longer T_1 than the Q⁴ silicons, and the spin-diffusion mechanism must be weak so as not to produce an average T_1 for both types of silicon. The large values of T_1 below T_g after heating can be explained in terms of a loss of water from the sample on heating. However, the high-temperature (above T_g) hysteresis must be due to some other mechanism; the most likely is the reduction of Fe³⁺ to Fe²⁺ (or Fe⁰) in the reducing atmosphere (Ar + 3% H₂) of the furnace. This reduces the moment on the iron and hence its effectiveness in causing relaxation. If the amount of reduction is small, this will have a large effect on the undoped sample with very little iron impurity and a much lesser effect on the doped sample, which is what is observed. T_1 data for doped and undoped samples of potassium tetrasilicate have been recorded by Liu¹¹ at 4.22 T. These data allow us to make some estimates¹² of the strength of the paramagnetic relaxation via values of T_1 measured at different magnetic fields. We estimate an electronic relaxation time (T_1) of 4.5×10^{-9} s at room temperature which would indicate a local electronic field of ~ 3.1 G and consequently a critical radius around each impurity of ~ 18 Å; this compares with an average impurity separation of 110 Å. However, the contribution of unknown types of impurity and paramagnetic species makes this a very rough estimate. If re-

(7) Cookson, D. J.; Smith, B. E. *J. Magn. Reson.* **1985**, *63*, 217–218.

(8) Gladden, L. F.; Carpenter, T. A.; Elliot, S. R. *Phil. Mag.* **1986**, *B53*, L81–L87.

(9) Wolf, D. *Spin Temperature and Nuclear Spin Relaxation in Matter*; Oxford University Press: Oxford, 1979.

(10) Richards, P. M. *Phys. Rev. B* **1978**, *18*, 6358–6371.

(11) Liu, S.-B.; Stebbins, J. F., unpublished data.

(12) Abragam, A. *The Principles of Nuclear Magnetism*; Oxford University Press: Oxford, 1961.

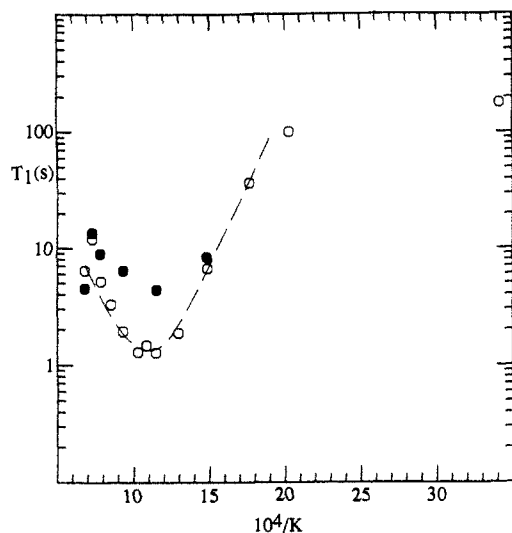


Figure 3. ²⁹Si T_1 versus inverse temperature for lithium orthosilicate/metasilicate mixture: data measured with increasing temperature (O); data measured on a second experimental run (●). The dashed curve represents a fit to a heteronuclear relaxation of silicon by lithium motion.

relaxation is via the paramagnetic impurities, then T_1 should be inversely proportional to the number of paramagnetic impurities per cm^3 (N) at all temperatures (for reasonably small numbers of impurities). The T_1 for the doped sample (500 ppm of Fe^{3+} , $N = 7.55 \times 10^{17} \text{ cm}^{-3}$) should be a factor of at least 10 shorter than an undoped sample with <50 ppm of Fe^{3+} ; in fact, the difference is about 4 at 1200 °C, a temperature at which the effects of impurities such as OH should have been removed.

Despite the inconsistencies in the exact nature of the interaction causing spin-lattice relaxation in these two silicate systems, the high values of the apparent activation energies measured from the slopes of the T_1 versus temperature curves indicate that they will be associated with motions which are important in the microscopic description of their macroscopic properties such as viscosity. The relatively high values of activation energy (138.6 and 181.3 kJ mol^{-1} for albite and potassium tetrasilicate, respectively) would not be involved in simply activating a mechanism analogous to relaxation by fixed paramagnetic impurities unless this activation energy was related to the breaking and re-forming of Si-O bonds. Obviously, creating a dangling bond would provide a paramagnetic relaxation mechanism, but in the case of elemental selenium¹³ (which forms molecular chains) when bond-breaking produces dangling bonds, the rapid increase in the relaxation rate is also accompanied by a large paramagnetic shift of the resonance. There appears to be only a slight shift of a few ppm even at the highest temperatures in the data here; either this effect is quite small in these systems or the shift is, more likely, due to a change in chemical shift.

The low-silica system lithium orthosilicate/metasilicate ($\text{Li}_4\text{SiO}_4/\text{Li}_2\text{SiO}_3$) has a better understood T_1 relaxation mechanism. It was chosen as an example of a low silica liquid which would melt at a reasonable temperature (1024 °C). However, this sample is a crystalline solid, whereas the other two samples were glasses. The T_1 versus temperature plot in Figure 3 shows the large difference in T_1 behavior compared with the high silica glasses. A distinct T_1 minimum is observed while the sample is still solid at ~ 600 °C. This is due to the high mobility of Li^+ in these structures; both ⁷Li and ⁶Li have a magnetic dipole moment so their motion through and within the structure can produce a fluctuating magnetic field which will relax the silicon nuclei in the silicate framework. This motion seems to begin above 200 °C and the solid curve in Figure 3 is a fit to the data assuming heteronuclear dipolar relaxation and an activation energy of $53.1 \pm 2.0 \text{ kJ mol}^{-1}$ measured from the low-temperature T_1 slope. The activation energy above the T_1 minimum is $76.0 \pm 3.4 \text{ kJ mol}^{-1}$.

(13) Warren, W. W.; Dupree, R. *Phys. Rev. B* **1980**, *22*, 2257-2275.

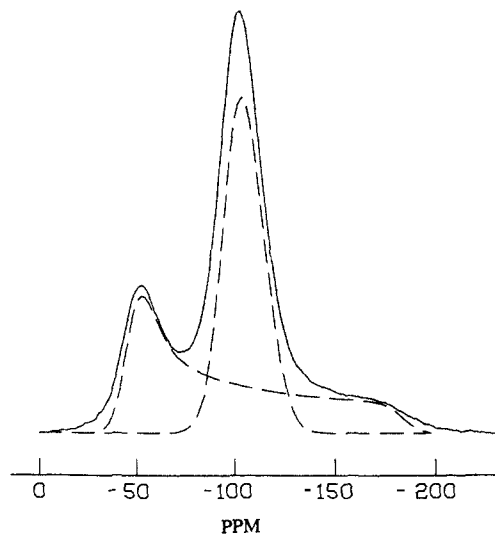


Figure 4. ²⁹Si NMR spectrum of potassium tetrasilicate glass (doped with 500 ppm of Fe_2O_3) at 20 °C: 128 pulses ($\pi/2$) with a delay of 300 s. The dashed lines show the two resonances (Q^3 and Q^4) which compose the total line shape.

Conductivity data¹⁴ on lithium orthosilicate give an activation energy of 84.4 kJ mol^{-1} and ⁷Li NMR data¹⁵ measured between room temperature and 500 °C a value of $50.6 \pm 6.1 \text{ kJ mol}^{-1}$. Thus it would appear that at temperatures above the T_1 minimum the Li^+ motion is predominantly a through-going diffusion (the type responsible for conductivity) and below the T_1 minimum a more localized motion. The agreement between the activation energies determined by ²⁹Si NMR and the ⁷Li NMR and conductivity data is good, and in addition the attempt frequency ($1/\text{correlation time at infinite temperature}$) from ²⁹Si NMR which lies between 1.42×10^{13} and $8.33 \times 10^{11} \text{ Hz}$ is consistent with the value of $1.11 \times 10^{12} \text{ Hz}$ obtained from the ⁷Li NMR data. The ⁷Li NMR data on Li_2SiO_3 ¹⁶ yield an activation energy of 78.0 kJ mol^{-1} for Li^+ diffusion which did not show a T_1 minimum over the temperature range studied (25–700 °C), and substantial ionic motion did not commence until ~ 400 °C.

It is significant that above the melting point of the eutectic composition (1024 °C) the T_1 decreases rapidly; this decrease was observed in both experimental runs, so it appears that another mode of relaxation is operating in the melt where the silicons in Q^0 and Q^2 sites are exchanging rapidly. The most likely mechanism will be similar to that operating in the more silica-rich melts discussed earlier.

Line Shapes. The ²⁹Si resonance in potassium tetrasilicate glass consists of two overlapping lines for silicons in Q^4 and Q^3 environments (Figure 4). The highly symmetric Q^4 site gives a relatively narrow line which is approximately Gaussian. The breadth is due to distributions in the Si-O-Si bond angle¹⁷ and, to a lesser extent, Si-O bond lengths. In the case of the static line shape, broadening due to a small amount of chemical shift anisotropy is also expected.¹⁸ In contrast, the Q^3 line shape is dominated by chemical shift anisotropy, showing a characteristic uniaxial powder pattern¹⁹ (there is some slight deviation from a perfect uniaxial pattern). The distributions of bond angle and length which broadened the Q^4 line serve only to smooth the line shape in the Q^3 case.

The line shape described above is maintained as the temperature of the sample is raised through the glass transition ($T_g \sim 500$ °C) with the only difference being a very slight sharpening of the

(14) Hu, Y.-W.; Raistrick I. D.; Huggins, R. A. *J. Electrochem. Soc.* **1977**, *124*, 1240-1242.

(15) Asai, T.; Kawai, S. *Solid State Ionics* **1982**, *7*, 43-47.

(16) Matsuo, T.; Ohno, H.; Noda, K.; Konishi, S.; Yoshida, H.; Watanabe, H. *J. Chem. Soc., Faraday Trans. 2* **1983**, *79*, 1205-1216.

(17) Smith, J. V.; Blackwell, C. S. *Nature (London)* **1983**, *303*, 223-225.

(18) Spearing, D. R.; Stebbins, J. F. *Am. Miner.* **1989**, *74*, 956-959.

(19) Bloembergen, N.; Rowland, T. J. *Acta Metall.* **1953**, *1*, 731-746.

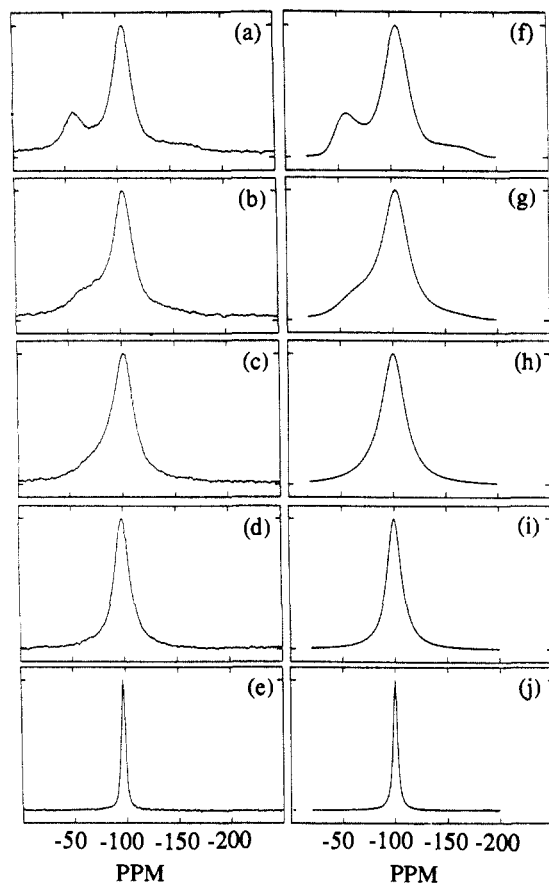


Figure 5. ^{29}Si NMR spectra (a–e) of potassium tetrasilicate glass and simulations (f–j). Spectra were recorded with 64 pulses ($\ll \pi/6$) and delays determined from the T_1 data at (a) 697 °C, (b) 774 °C, (c) 800 °C, (d) 847 °C, (e) 997 °C. Simulations of these spectra were judged “by eye” to be the best match with exchange rates of (f) 2000 Hz, (g) 10 000 Hz, (h) 25 000 Hz, (i) 50 000 Hz, (j) 500 000 Hz.

powder pattern at 600 °C from that at room temperature. Only at 700 °C do the motional narrowing effects commonly observed in NMR at high temperature commence. The line shape continues to narrow until at 950 °C a single narrow line is observed. The existence of the single narrow line is confirmation of the result of Liu et al.³ that a process analogous to chemical exchange is taking place and silicon atoms are experiencing Q^3 and Q^4 sites at a rate which is significantly greater than the difference in NMR frequencies of the two sites. The line shapes in Figure 5a–e show the various degrees of narrowing at some of the temperature steps.

The data in Figure 5 form the basis for a line-shape analysis since the resonances for the each site are so distinct. The static albite line shape is broad and featureless over most of the temperature range and only begins to narrow at ~ 1000 °C. The fact that five silicon environments $Q^4(nAl)$ ($n = 0, 1, 2, 3, 4$) are possible in a glass sample means that line-shape analysis was not suitable for the albite sample. The advantage of a line-shape analysis is demonstrated by the results of the previous section regarding T_1 relaxation where very small changes in the amounts or nature of an impurity can greatly influence the relaxation. This may mean, in the worst case, that any activation energies inferred from T_1 data cannot be uniquely attributed to the motions of interest but may be due to some activated process related to the impurity.

The analysis of chemically exchanging line shapes in liquid-state NMR is well developed.²⁰ In the solid state there have been several elegant studies of molecular rotations, jumps, and flips in crystals.^{21,22} In these cases the symmetry of the molecules

involved simplified the problem, and generally the line-shape analysis allowed discrimination between models of discrete molecular jumps and rotational diffusion. The principle of the calculation of line shapes in the chemical exchange regime (where the exchange is of the order of the frequency difference between resonances) is detailed in the texts by Abragam¹¹ and Mehring²³ (for solids). In essence, the equation of motion of the magnetization (M) can be written in terms of the frequencies of individual lines (ω_j) in the spectrum, a T_2 term (independent of exchange effects), and an exchange term, \prod_{jk}

$$dM_j(t)/dt = i\omega_j M_j(t) - (1/T_2)M_j(t) + \sum_k \prod_{jk} M_k(t) \quad (1)$$

The last term in (1) can be expressed as an exchange matrix \prod describing the mode of site exchange and is dependent on the model chosen. For the case of all sites (N) exchanging at a rate of K (τ^{-1}), the exchange matrix will have the elements

$$\prod_{jk} = K(1 - N\delta_{jk}) \quad (2)$$

Since the probability of jumping to any other site is K , the off-diagonal elements ($\delta_{jk} = 0$) are one, and the diagonal elements ($\delta_{jk} = 1$) will be $-(N-1)$ to ensure $\sum_{j,k} \prod_{jk} = 0$. The full matrix solution of (1) for the line shape is

$$M(\omega) = A(\omega)^{-1}M(t=0) \quad (3)$$

where $A = i(\omega\mathbf{1} - \omega) - \prod$, ω includes the T_2 term, and $\mathbf{1}$ is the unit matrix. If the initial magnetization $M(t=0)$ is the initial probability vector, W , the line shape, $g(\omega)$, then becomes

$$g(\omega) = \mathbf{1} \cdot A(\omega)^{-1} \cdot W \quad (4)$$

This expression is the basis of calculations of line shapes in the presence of chemical exchange.

In most previous studies in the solid state the exchange has been between a few sites related by symmetry making the matrix A small. The inverse of A has to be computed so the calculation is straightforward, although, because the samples were usually powdered solids, the averaging over all possible orientations was a lengthy process. Previous motions studied have been rotations or jumps about molecular axes which involve a well-characterized motion. In the rapid exchange limit the chemical shift anisotropy in the rigid situation becomes modified under motion usually by acquiring a new unique chemical shift anisotropy axis coinciding with the axis of rotation. The situation with a liquid in the exchange region (above its glass transition) is substantially different from the situation just described in a crystalline solid. The powder pattern of the glass is retained up to 200 °C above T_g ; however, the modes of motion which will narrow this powder pattern and eventually result in a single narrow line must include Q^3 and Q^4 silicons exchanging sites (breaking Si–O bonds in the process) and also reorientation of a Q^3 or Q^4 with respect to the external magnetic field, thereby changing its resonance frequency. It may not be possible to separate these two processes from the data, although work is in progress.²⁴ The approach here was to treat the problem as one of N site exchange where N was large enough to simulate the room-temperature spectrum of the glass using an analytic expression for N site exchange²³ and an exchange rate of zero.

$$g(\omega) = (1/N)[1/(1 - KL)] \quad (5)$$

where

$$L = \sum_{j=1,N} [i(\omega - \omega_j) + (1/T_2) + NK]^{-1} \quad (6)$$

In this analysis 15 000 sites were distributed equally between Q^3 and Q^4 sites; 7500 Q^3 frequencies were generated by taking that many angular steps through the expression for the uniaxial powder pattern with values of σ_{parallel} and $\sigma_{\text{perpendicular}}$ determined from the room-temperature spectrum and a single value of T_2 determined as the inverse of the limiting line width of the NMR

(22) Spiess, H. W. *Chem. Phys.* **1974**, *6*, 217–225.

(20) Kaplan, J. I.; Fraenkel, G. *NMR of Chemically Exchanging Systems*; Academic Press: New York, 1980.

(21) Wemmer, D. E. Ph.D. Thesis, University of California, Berkeley, 1978.

(23) Mehring, M. *Principles of High Resolution NMR in Solids*; Springer-Verlag: Berlin, 1983.

(24) Farnan, I.; Stebbins, J. F.; Williams, E. H. Abstract w. Program; 30th Experimental NMR Conference, 1989.

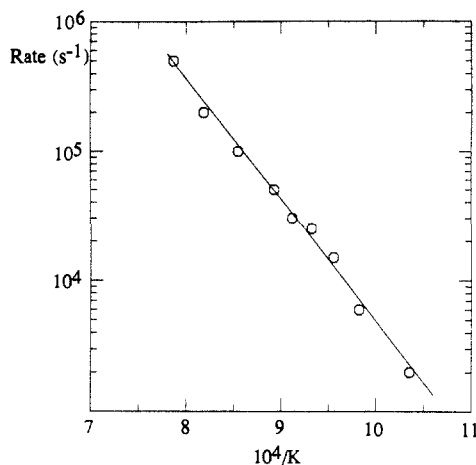


Figure 6. Plot of the simulation exchange rate against inverse temperature for doped potassium tetrasilicate glass. The slope yields an activation energy of $179.4 \pm 5.4 \text{ kJ mol}^{-1}$.

probe ($T_2 = 3.5 \text{ ms}$). The Q^4 frequencies were generated by having a Gaussian distribution of 7500 occurrences of 150 frequencies around the Q^4 peak position. It was necessary to introduce some Gaussian distribution of uniaxial parameters into the Q^3 sites to simulate the randomness of the glass. The initial conditions were then used to simulate the spectra at different temperatures. The results can be seen in Figure 5, f–j. The general features of the low-temperature line shapes (697–774 °C) are reproduced well with some slight discrepancy in the width of the Q^4 peak (slightly too wide in the simulation) which may be due to the assumption of a single T_2 for both sites or may reflect a more ordered distribution of Q^4 angles at the higher temperatures, although this is unlikely as previous work⁵ has indicated a greater degree of randomness in glasses with higher T_g 's. At higher temperatures the line widths and shapes match very well, the only discrepancy being the position of the narrowed peak which is $\sim 2 \text{ ppm}$ from the experimental peak, this may be due to a different "instantaneous" chemical shift anisotropy for the sites at 1050 °C compared with room temperature; in fact, it would be surprising if this were not so. The rates from the simulations at each temperature can be used to calculate an activation energy for the exchange process. The plot of $\log \text{rate} \nu 1/\text{temperature}$ for the potassium tetrasilicate line-shape simulations are shown in Figure 6; the activation energy is found to be $179.4 \pm 5.4 \text{ kJ mol}^{-1}$. This result agrees with the activation energy previously determined from the T_1 data.

The ²⁹Si line-shape data for the lithium orthosilicate/metasilicate system are shown in Figure 7. The broad featureless line observed at room temperature is due to the dipolar broadening of silicon by lithium and completely masks the range of Q^2 and Q^0 silicon sites indicated by the structures of the two components of this sample. As it is known from the T_1 data that Li ion motion begins to be detectable at about 200 °C, we might expect the dipolar interaction to be removed by this motion and to see a narrowed spectrum at 401 °C. The spectrum observed at 401 °C is unusual since the removal of the dipolar broadening might be expected to leave the powder patterns for the Q^0 and Q^2 silicon sites in the material. However, the slow-spinning room-temperature MAS spectra of this sample (spectrum not shown) allows the chemical shift anisotropy parameters to be estimated using the Herzfeld and Berger approach;²⁵ these parameters are $\sigma_{11} = 30 \text{ ppm}$, $\sigma_{22} = -66 \text{ ppm}$, $\sigma_{33} = -100 \text{ ppm}$ for the Q^0 sites and $\sigma_{11} = -15 \text{ ppm}$, $\sigma_{22} = -68 \text{ ppm}$, $\sigma_{33} = -144 \text{ ppm}$ for the Q^2 sites. It can be seen from the 401 °C spectrum that it is narrower than the powder patterns which would be generated by these parameters. The explanation must be that the silicons are experiencing a reduced chemical shift anisotropy due to the motion of the lithium ions. When the temperature is increased further, the mode

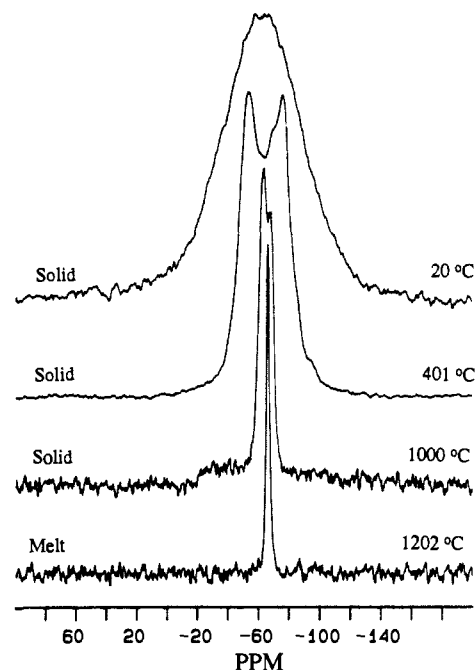


Figure 7. Variable-temperature ²⁹Si NMR spectra of the lithium orthosilicate/metasilicate mixture. Spectra were acquired using $< \pi/6$ pulses and delays determined from the T_1 data. Typically, narrow spectra required 64 pulses and broader spectra 500 pulses. The line broadening used in processing each spectrum was less than 10% of the total line width.

of lithium motion changes to a more through-going diffusion as mentioned earlier in connection with the T_1 results. This effect is seen in the ²⁹Si spectrum at 1000 °C as a further narrowing, and the chemical shift of the orthosilicate Q^0 now has its isotropic value (-65.2 ppm). Apparently, the Li^+ ions are moving so rapidly that the SiO_4 tetrahedra with no bridging oxygen bonds have, on the average, no orientation dependence in their chemical shift. The metasilicate (Q^2) silicons must retain their two bridging oxygens if the sample is to remain a solid (which it is), but the other two bonds per tetrahedra are breaking and re-forming rapidly on the NMR time scale, this produces a line shape which has a hint of anisotropy to the positive side of the spectrum. Once the sample is molten ($T_m = 1024 \text{ °C}$), a single narrow line is observed indicating rapid exchange of Q^0 and Q^2 (and almost certainly Q^1) sites as in the higher silica content melts. The spectrum shown at 1202 °C has a shift of -67.1 ppm which is different from the weighted mean of the two isotropic shifts (-71.7 ppm); that is more positive (deshielded) than expected, the same direction as the high-temperature shift of the potassium tetrasilicate line.

Discussion

The most significant results of this work come from the higher temperature ²⁹Si NMR spectra. These show that the lifetime of a silicate tetrahedron in the melt is short on the NMR time scale because only one line is observed in the spectra of samples where, by stoichiometry, more than one silicon environment must exist. This is true for samples of greatly differing silica contents and shows that even when a silicate system contains a large proportion of weak bonds, the Si–O bonds in the system are breaking and re-forming rapidly. The registration of line-shape data with good signal to noise has allowed line-shape analysis to give the rate of the bond-breaking process at various temperatures. The inverse of this rate gives the average lifetime of a particular silicate tetrahedron in the melt, so at 1000 °C the lifetime of silicate tetrahedra in potassium tetrasilicate is $\sim 2 \mu\text{s}$. The activation energy derived from the line-shape analysis can be used to extrapolate back to the glass transition (T_g) to give the rate at that temperature; for potassium tetrasilicate this is $\sim 500 \text{ °C}$ which corresponds to a rate of $\sim 9 \text{ Hz}$, a value which agrees with conventional belief about the rate of motion at the glass transition. The previous ²⁹Si NMR data on silicate melts^{2,3} relied on the activation energies measured from T_1 versus $1/\text{temperature}$ plots

(25) Herzfeld, J.; Berger, A. E. *J. Chem. Phys.* 1980, 73, 6021–6030.

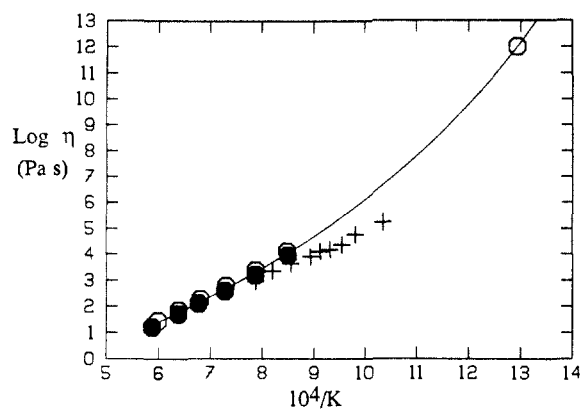


Figure 8. Plot of log viscosity (η) against inverse temperature for $\text{K}_2\text{O-SiO}_2$ using the data of Shartsis et al.: (O) 18.6 mol % K_2O , (●) 21.4 mol % K_2O . (+) are the viscosities determined from the NMR results (see text) for potassium tetrasilicate ($\text{K}_2\text{Si}_4\text{O}_9$) glass.

and extrapolated from the correlation time at the T_1 minimum ($1/\omega_0$), which is of the order of 5 ns, to get the rate of motion at T_g . Consequently, the values obtained were a factor of 10^3 higher than those obtained here. Although not always possible, the line-shape analysis approach does provide a method with a greater degree of confidence than the relaxation time treatment since the latter may be affected by very subtle changes in the nature or concentration of impurities.

The activation energy derived for potassium tetrasilicate from the line-shape analysis can be compared with the activation energy calculated from the data of Shartsis et al.²⁶ for the viscosity of $\text{K}_2\text{O-SiO}_2$ compositions at various temperatures. Combining the data for the 18.6 and 21.4 mol % K_2O compositions gives an activation energy of $201.0 \pm 6.1 \text{ kJ mol}^{-1}$. This is remarkably close to the value obtained in this study for silicon site exchange. This implies that NMR is coming close to detecting the fundamental step in flow, the activation energy of which probably determines the viscosity of a silicate liquid. The viscosity of silicate liquids are usually measured in high and low viscosity regions using bending beam and concentric cylinder apparatus, respectively; values for intermediate viscosities are very rare. The data in each region are usually describable by an Arrhenian activated process, but the total viscosity temperature curve cannot be described by an Arrhenian relationship. As it is generally believed that silicate melts will have a viscosity of about 10^{12} Pa s at T_g , this constraint may be used to fit low viscosity data to a total curve if the high viscosity data is not available for a particular composition. Figure 8 shows the Shartsis et al. data fitted to an expression of the form

$$\log \eta = A + B/(T - T_0) \quad (7)$$

including the value of 10^{12} Pa s for the viscosity at the glass transition and a value of $435 \text{ }^\circ\text{C}$ for T_0 which can be thought of as the temperature at which the glass will have infinite viscosity. The Stokes equation relating the diffusivity, D , of rigid spheres of radius, a , to viscosity, η

$$D = kT/6\pi a\eta \quad (8)$$

can be combined with the Einstein-Smolukowski relationship between a characteristic diffusion time, τ , diffusivity, and characteristic distance, d

$$D = d^2/2\tau \quad (9)$$

If the inverse of the rate determined at each temperature is used as the characteristic time and the average Si-Si separation as the characteristic distance (3.1 Å), then the calculated diffusivities may be used to crudely estimate the viscosity. The data in Figure 8 show that the agreement of this rather crude calculation is remarkable, considering that viscosity of silicates can vary by over

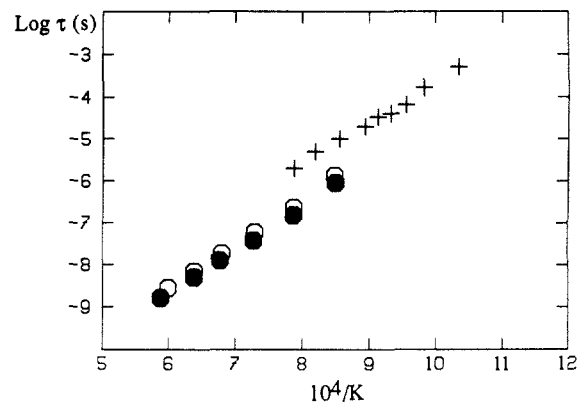


Figure 9. Plot of relaxation time against inverse temperature: Shear relaxation times (τ_s) for 18.6 mol % K_2O (O) and 21.4 mol % K_2O (●) for the system $\text{K}_2\text{O-SiO}_2$ and time constants of the exchange from the variable-temperature NMR data for $\text{K}_2\text{Si}_4\text{O}_9$ (+).

13 orders of magnitude across the temperature and composition ranges of interest to geologists and glass technologists. The viscosities determined from the NMR data appear to approach the high-temperature data asymptotically, which may be interpreted as the characterization of one of the limits of a range of configurational changes which contribute to the viscosity. As a silicate liquid is thought to be far too complex to be describable by a simple rigid-sphere model of diffusion and viscosity, it would be advantageous to have some other means of relating the rate of exchange determined by NMR to the time scale of processes occurring in the liquid. One parameter which may well provide this relationship is the shear relaxation time, τ_s . Dingwall and Webb²⁷ have pointed out that the shear relaxation time can be determined from the zero-frequency shear viscosity and the shear modulus at infinite frequency (G_∞) using only the viscosity data and an average value of G_∞ . Because G_∞ remains fairly constant compared with the shear viscosity over a large temperature range, the shear relaxation times for a large number of silicate systems can be calculated via the Maxwell equations for viscoelastic behavior (eq 10) using only the viscosity data and an average value

$$\tau_s = \eta_s/G_\infty \quad (10)$$

of $\log G_\infty = 10.0$. These shear relaxation times are plotted in Figure 9 for the $\text{K}_2\text{O-SiO}_2$ viscosity data with the NMR rate data. The overlapping values are within half a log unit of each other with very good agreement between the slopes. The good agreement between the NMR derived properties and the bulk measurements for potassium tetrasilicate in the low to medium viscosity region may provide an insight into the total temperature viscosity curve. It was mentioned previously that the simulations of the line-shape data gave a width for the Q^4 peak which was slightly too wide at the lowest temperatures. In the simulation procedure an homogeneous line shape was used; i.e., all lines could exchange with all other lines. If there was some preferential "self-exchange" among the Q^4 and Q^3 sites then the Q^4 line would narrow more rapidly for the same exchange rate than the total $Q^3 + Q^4$ line shape because it covers a much smaller frequency range. Consequently, it may be this process which dominates the viscosity at lower temperatures, gradually evolving to a complete exchange process at the highest temperatures. Progress is being made to evaluate the contributions of different rates of exchange to the experimental line shapes using more sophisticated exchange models.²⁴ The "self-exchange" may involve the transitory distortion of Si-O bonds with the atoms not necessarily returning to their original positions after the event, it could then be conceivable that there would be some low probability of complete bond breaking and a flow event occurring resulting in the poor fluidity of these melts near the glass transition. The NMR T_1 data for potassium tetrasilicate and albite suggest that motions which are of the order of 1 kHz exist at T_g and are responsible for the spin-lattice

(26) Shartsis, I.; Spinner, S.; Capps, W. *Am. Ceram. Soc. J.* **1952**, 155-160.

(27) Dingwall, D. B.; Webb, S. L. *Phys. Chem. Miner.* **1989**, 16, 508-516.

relaxation. To speculate, the T_1 relaxation could be viewed as a higher frequency local motion and the exchange between Q species as a lower frequency through-going motion somewhat analogous to the two modes of local and diffusive motion observed for the lithium silicate sample. Although the frequency of motion causing the T_1 is known, the exact interaction responsible is the subject of speculation. The idea that the increased likelihood of a silicon having a paramagnetic neighbor is causing the T_1 relaxation above T_g is the most convincing. The importance of T_1 relaxation by fixed paramagnetic impurities in insulating materials was realized from the earliest days of solid-state NMR;²⁸ the measured T_1 's could not be explained unless there was some mechanism to transport spin energy to the paramagnetic impurities. The process could be explained using a diffusion equation for the transport of polarization,^{29,30} i.e., spin diffusion, D_s . The extension of this process for fast ion conductors where particle diffusion, D_p , was also present was made by Richards,¹⁰ in which the diffusion term became dependent on the distance (r) of a nucleus from the paramagnetic impurity. This gave a term $D(r)$ for the diffusion coefficient which was $D_p + D_s$ when $r > b$ and D_p when $r < b$, b being the radius around an impurity where the influence of the electronic field quenches spin diffusion. The quantity $W\tau_c$ compares the hopping rate of the diffusing nucleus (W) with the electronic relaxation time (τ_c). If $W\tau_c \gg 1$, then the effective fluctuation rate is just W . This is analogous to the situation of paramagnetic relaxation in solutions or nonviscous liquids where characteristic self-diffusion times are of the order of 10^{-11} s. In these viscous silicate liquids the situation is more complicated because the resonant nuclei and the paramagnetic impurities are both diffusing almost certainly at different rates, and rates which will range from very much less than to not significantly greater than the estimated electronic relaxation times of the impurity. Consequently a detailed theoretical treatment of this type of situation is required.

The agreement of the activation energy measured from the T_1 relaxation curve (181.3 ± 8.6 kJ mol⁻¹) and that from the line-shape analysis (179.4 ± 5.4 kJ mol⁻¹) of potassium tetrasilicate would suggest that either the agreement is coincidental or that some indirect process is controlling both mechanisms, mechanisms which must be different because they have different rates. The fact that the silicon seems so intimately involved in the fundamental step in viscous flow would suggest that there must be some cooperative motion of a few atoms in order to transfer a silicon from one site to another. The necessary opening of the structure as some atoms move together to change a Q³ to a Q⁴ site could allow impurities to diffuse through the structure and cause the rapid increase in relaxation. The activation energy for diffusion of trace amounts of ferric ions in a high silica melt has been measured as 157 kJ mol⁻¹ by a potential sweep method.³¹ This

would at least be consistent with a process of this sort. If the diffusion coefficients for silicon calculated from the NMR data and for Fe³⁺ extrapolated from high temperature are compared, then at 1000 °C $D(\text{Si}) = 2.4 \times 10^{-10}$ cm² s⁻¹ and $D(\text{Fe}^{3+}) = 4.6 \times 10^{-8}$ cm² s⁻¹; this shows a factor approaching the 10³ difference between the rates of the two processes.

It is often proposed³² that the fundamental step in viscous flow in silicates is the movement of a single oxygen atom, i.e., oxygen diffusion. It may be envisaged that the same arguments for a cooperative process of Q species exchange and Fe³⁺ diffusion could be applied to oxygen diffusion. There is conflicting evidence from oxygen diffusion measurements^{32,33} using ¹⁸O labeling as to whether a single oxygen atom is the diffusing species. The problem lies in the simplicity of the Eyring model used to estimate the fundamental distance involved, which is then interpreted in terms of the diameter of an O²⁻ ion or a SiO₄⁴⁻ ion. One possible way of resolving this, using NMR experiments, is to perform line-shape studies on ¹⁷O-enriched samples.

The analysis of NMR line shapes at high temperature in silicates and oxides, of which this study is the first example, should open up an area of study previously undeveloped because of perceived technological difficulties. Line-shape analysis in terms of chemical exchange allows local and through-going modes of motion to be distinguished, the separation of which has hampered more traditional relaxation time studies at high temperature. Future experiments could include in situ observations of the dynamics of nucleation and crystallization and solid-solid phase transitions as well as further investigation of silicate melts.

Conclusions

The lifetime of a silicate tetrahedral species in a melt is short on the NMR time scale, indicating the presence of chemical exchange processes. In addition NMR line-shape data of sufficient quality can be obtained to model exchange processes and relate the rate to the time scale of bulk properties of the melt. The activation energy of the exchange process is in good agreement with measured activation energy for viscous flow. In general, NMR measurements of silicates at higher temperatures have the possibility of providing the sort of dynamic information previously obtained in NMR studies of organic polymers.

Acknowledgment. This work was supported by NSF Grants EAR 8707175 and EAR 85-53024, and the PYI program. The authors thank Evan Williams for helpful discussions regarding chemical exchange. Funding for the spectrometer was provided by the National Science Foundation (Materials Research Laboratories and Earth Sciences Instrumentation and Facilities Programs), the Pew Memorial Trust, and a gift from Varian Associates.

(28) Bloembergen, N. *Physica* **1949**, *15*, 386-426.

(29) DeGennes, P. G. *J. Phys. Chem. Solids* **1958**, *7*, 345-350.

(30) Rorschach, H. E. *Physica* **1964**, *30*, 38-48.

(31) Takahashi, K.; Miura, Y. *J. Non-Cryst. Solids* **1980**, *38*, 39, 527-532.

(32) Shimizu, N.; Kushiro, I. *Geochim. Cosmochim. Acta* **1984**, *48*, 1295-1303.

(33) Dunn, T. *Geochim. Cosmochim. Acta* **1982**, *46*, 2293-2299.